ELSEVIER

Contents lists available at ScienceDirect

# **Hybrid Advances**

journal homepage: www.journals.elsevier.com/hybrid-advances





# Theoretical and computational exploration of electronic structure, optical properties, open circuit voltage, and toxicity of perovskites solar Cell: $(Cs_2SiX_6, X = Cl, Br, and I)$

Md. Hazrat Ali <sup>a</sup>, Halima Khatun <sup>a</sup>, M.S.S. Khan <sup>a</sup>, Shuva Roy <sup>a</sup>, Shubha Roy <sup>a</sup>, Ridoy Hossain <sup>a</sup>, Md. Robiul Mia <sup>a</sup>, Ashiqur Rahman Khan <sup>a</sup>, Syed Arfin Hussain <sup>a</sup>, Md. Bayejid Hossen <sup>a</sup>, Md. Barkat Ullah Khan <sup>a</sup>, Abdul Kaiyum <sup>b</sup>, Md Tauhidul Karim <sup>c</sup>, Unesco Chakma <sup>a,e</sup>, Ajoy Kumer <sup>d,\*</sup>

- <sup>a</sup> Department Electrical and Electronic Engineering, European University of Bangladesh, Gabtoli, Dhaka, 1216, Bangladesh
- <sup>b</sup> Department of Physics, Jahangirnagar University, Savar, Dhaka, Bangladesh
- <sup>c</sup> Department Civil Engineering, European University of Bangladesh, Gabtoli, Dhaka, 1216, Bangladesh
- d Laboratory of Computational Research for Drug Design and Material Science, Department of Chemistry, College of Arts and Sciences IUBAT-International University of Business Agriculture and Technology, 4 Embankment Drive Road, Sector 10, Uttara Model Town, Dhaka, 1230, Bangladesh
- e School of Electronic Science and Engineering, Southeast University, Nanjing, PR China

### ARTICLE INFO

Keywords:
Band gap
Density of states
Perovskite
Photovoltaic devices
Dielectric function

### ABSTRACT

Perovskites are presently being considered as a feasible choice for hole-transport materials in photovoltaic devices. One material that stands out among the options is Cs<sub>2</sub>SiX<sub>6</sub>, where X indicates Cl, Br, and I. This material is of special interest due to its potential as a lead-free alternative, offering a variety of halide options. Moreover, several experimental inquiries have exhibited favorable outcomes; nevertheless, their theoretical or computational framework is limited and insufficient. As a result, the present investigation has opted for the crystal Cs<sub>2</sub>SiX<sub>6</sub> and synthesized Cs<sub>2</sub>SiX<sub>6</sub>, Cs<sub>2</sub>SiCl<sub>6</sub>, Cs<sub>2</sub>SiBr<sub>6</sub> and Cs<sub>2</sub>SiI<sub>6</sub> to examine their electronic structures and optical properties using the DFT functional. The electronic structure of Cs<sub>2</sub>SnBr<sub>6</sub>, was calculated using GGA with PBE functional, yielding a band gap of 2.434 eV. It should be noted that the experimental value of Cs<sub>2</sub>SnBr<sub>6</sub> was 2.450 eV. Furthermore, the band gaps of Cs<sub>2</sub>SiCl<sub>6</sub>, Cs<sub>2</sub>SiBr<sub>6</sub>, and Cs<sub>2</sub>SiI<sub>6</sub> were calculated by GGA with PBE to be 1.540 eV, 1.291 eV, and 0.261 eV, respectively. In this study, various pseudopotential techniques are employed to investigate the electrical structures. Five different densities functional theory (DFT) functionals are utilized to determine the most accurate functional. Additionally, the study focuses on the LDA, a unique junction photovoltaic material. In addition, the six optical properties, specifically absorption, reflection, refractive index, conductivity, dielectric function, and loss function, are calculated to provide additional understanding of material qualities in the presence of visual evidence. The utilization of the Density of States (DOS) and the Partial Density of States (PDOS) was employed in order to calculate the electronic structure and bonding properties. For a material to effectively operate as a single-junction photovoltaic, it is imperative that its band gap remains within the specified range of 0.261-1.540 eV. The materials being discussed are conserved within this designated range and employed for their intended purposes. In summary, our research yields strong evidence suggesting that the aforementioned materials lack carcinogenic qualities and demonstrate only moderate degrees of toxicity. In sharp contrast, it has been observed that perovskites containing lead exhibit considerably higher levels of toxicity.

### 1. Introduction

The scientific and research communities have shown considerable

interest in Perovskite materials owing to their potential utility in thirdgeneration solar devices. Moreover, the investigation of perovskite cells holds significant importance within the framework of the prevailing

E-mail addresses: kumarajoy.cu@gmail.com, ajoy.chem@iubat.edu (A. Kumer).

https://doi.org/10.1016/j.hybadv.2023.100084

<sup>\*</sup> Corresponding author.

energy crisis [1,2]. Despite the extensive research and development of various perovskite materials for their efficient utilization, certain limits have been found. The principal considerations pertaining to the advancement of innovative perovskite materials, encompassing cells, revolve around the issues of toxicity and efficiency. Organic-inorganic hybrid perovskites have gained recognition for their favorable attributes in terms of toxicity and environmental sustainability, rendering them a feasible choice for the utilization in optoelectronic device applications [3], The organic ligand of methylamine was employed as a distinctive organic high-end component [1,2]. The aforementioned properties, namely high absorption coefficients, long carrier diffusion lengths, and cost-effective processing expenses, are distinctive characteristics of the subject under consideration. [3], where the lead was the other end as metal [4]. In addition, they showcase economically viable equipment for prospective future utilization, along with straightforward preparation methodologies [8]. Meanwhile, significant progress has been made in the utilization of lead halide perovskites for various applications such as photovoltaic cells [9], light emitting diodes [10], lasers [11], and photo detectors capable of detecting near infrared, ultraviolet, and visible light [12].

Recently, there are some reports on metal halide based crystal ( $Cs_2SnX_6$ ; X = halogen atoms) type which is able to absorb light in the visible to infrared (IR) region, The discovery has engendered a sense of optimism regarding the potential for the advancement of chemically stable materials that are in accordance with principles of environmental sustainability [5]. As a result, it produces low toxicity or not easily degradation. One of the crystal of Cs<sub>2</sub>SnX<sub>6</sub>,Cs<sub>2</sub>SnI<sub>6</sub>, with a cubic crystal structure having +4 oxidation state, is regarded as a potential candidate for new applications in perovskite solar cells (PSCs) [6]. The efficacy of these applications is primarily determined by the band gap, which directly controls the absorption of light and must be considered for the construction of optoelectronic devices. However, the diffused reflectance measurements of Cs<sub>2</sub>SnI<sub>6</sub> shows an optical band gap in 1.25-1.30 eV for comparison to the thin film band gap with 1.60 eV. A functional can be characterized as a mathematical mapping that operates on a function, with the Density Functional Theory (DFT) serving as a specific functional that operates on the basis of the electron density with respect to both spatial and temporal variables [15-17]. The utilization of electron density in Density Functional Theory (DFT) distinguishes it from Hartree-Fock theory, as it is intimately correlated with the many-body wavefunction [18,19]. The application of several functionals with different correlation approximations in density functional theory (DFT) led to a significant discrepancy between the experimentally measured value and the expected direct transition with a band gap (varying from 0.13 to 1.26 eV) [20]. Furthermore, this particular class of compounds demonstrates the capability to propagate through N-type semiconductor materials that are distinguished by their heightened electrical conductivity, substantial absorption capability, and resilient moisture stability [7]. Secondly, the Cs<sub>2</sub>SnI<sub>6</sub> has higher air stability than CsSnI<sub>3</sub>due to the tetravalent chemical nature of Sn. A number of transition metals exhibit stable +4 oxidation states and possess either non-toxic properties or demonstrate minimal levels of toxicity. This characteristic has paved the way for the discovery and exploration of halide perovskites that exhibit favorable properties, such as by replacing the Sn<sub>4</sub><sup>+</sup> in Cs<sub>2</sub>SnI<sub>6</sub> with appropriate transition-metal cations [8]. Previously, Sakai et al.2017 confirmed this when they investigated to Cs<sub>2</sub>PdBr<sub>6</sub> as a novel perovskite for use in PSCs [9]. The optical band gap of Cs<sub>2</sub>PdBr<sub>6</sub> calculated from optical absorption was at 1.60 eV [9].Next, Ju et al.2018carried out an integrated experimental and theoretical study of Ti-based vacancy-ordered double perovskites (DPs)  $A_2TiX_6$  (A = K+, Rb+, Cs+ In+; X = I, Br, or Cl) and Cs<sub>2</sub>TiIxBr<sub>6</sub>-x, conveying a suitable band gap in from 1.38 eV to 1.78 eV range for photovoltaic applications [10]. According to Zhao et al.2018, who studied the Cs<sub>2</sub>BX<sub>6</sub> family of vacancy-ordered DPs (B = Pd, Sn, Ti, Te; X = Cl, I), the compounds demonstrated a wide range of electronic structures and optical characteristics. [11]. A group of researchers used the hybrid functional (HSE06) to computationally study

compounds of the type  $A_2MX_6$  (A = K, Rb, and Cs, M = Sn, Pd, Pt, Te, and X = I), reporting the band gap and effective mass change as the A-site cation changes from K to Rb to Cs [12]. There is a noticeable lack of scholarly literature concerning the examination of band gaps and optical properties, which are crucial for understanding their intrinsic attributes, practical uses, and potential environmental hazards. The objective of this study is to perform a comparative analysis by employing computational screening and theoretical evaluation of several density functional theory (DFT) functionals using different basis sets. As the DFT is one of the reliance and the most acceptable functional to investigate the electronic and optical nature of A2MX6 type crystals. In our study, the DFT has been used to investigate new variants of the A2BX6 family for becoming single or double perovskites with possible A = Cs; B=Si; and X = Cl, Br, and I. The focus of this study revolves around the application of various metal substitutions within the field of photovoltaics and optoelectronics. Before delving into the examination of the electrical configuration and optical properties of these compounds, it is crucial to analyze their structural characteristics and determine the most stable structural configuration.

To find new materials for perovskite solar cells, the behavior of the associated Lead-Free Halide perovskite solar cell is established and related to the impact of the halogen atom on the electronic structure, DOS, PDOS, and optical properties of  $Cs_2SiCl_6$ ,  $Cs_2SiBr_6$  and  $Cs_2Sil_6$  crystals. In addition, we also report on the open circuit voltage  $(V_{oc})$  and the elastic constant stability of these compounds by calculating their formation energies. The present study has assessed the toxicity levels by analyzing the provided reports.

These compounds' unique properties can be leveraged in innovative solar cell architectures, including tandem cells, quantum dot-sensitized solar cells, and other novel device concepts that capitalize on their optoelectronic characteristics.

Theory and Experiment Synergy: The combination of theoretical calculations and experimental characterizations can elucidate the relationship between band structure, DOS, and optical properties. This synergy can guide material design and optimization for enhanced solar cell performance.

# 2. Computational methods

The GGA with PBE method was used to structurally optimize the  $Cs_2SnI_6,\ Cs_2SiCl_6,\ Cs_2SiBr_6,\ and\ Cs_2SiI_6crystals.$  For simulation, the convergence criterion for the force between atoms was at  $2\times 10^{-6}$  eV/atom,  $1\times 10^{-5}\ A^\circ$  acting the maximum displacement, and  $1\times ^{10-5}\ eV/$ atom was accounted to the total energy. The same condition was also applied to the  $Cs_2SnI_6,\ Cs_2SiCl_6,\ Cs_2SiBr_6,\ and\ Cs_2SiI_6\ systems,\ keeping the cut-off at 523 and the k-point at <math display="inline">4\times 4\times 2$ . The investigation utilized several pseudopotential techniques, including OTFG Ultra soft, OTFG norm conserving, Ultra soft, and Norm conserving, in order to optimize and identify the best appropriate strategy for attaining optimization. Using the same condition, the GGA with PBE, GGA with RPBE, GGA with PW9, GGA with WC, and GGA with PBE\_{SOL}\ methods were applied to calculate the electronic structure. Finally, LDA with CA-PZ was applied to determine the electronic structure and optimization.

The structural, electronic, and optical properties of  $Cs_2SnI_6$ ,  $Cs_2SiCl_6$ ,  $Cs_2SiBr_6$ , and  $Cs_2SnI_6$  were designed to simulate using the  $2\times1\times1$  cell models shown in Fig. 1(a), (b), 1(c), and 1(d), respectively. In order to determine the electronic structure of the crystals of  $Cs_2SnI_6$ ,  $Cs_2SiCl_6$ ,  $Cs_2SiBr_6$ , and  $Cs_2SiI_6$ , the method of GGA with PBE was first applied using the CASTEP code from Material Studio 8.0 [13–17].Following that, the calculation of the density of states and optical properties was performed using the same set of parameters. We used the stress-strain method to calculate the elastic stiffness constants of  $Cs_2SnI_6$ ,  $Cs_2SiCl_6$ ,  $Cs_2SiBr_6$ , and  $Cs_2SnI_6$  at zero pressure. The application of the generalized gradient approximation (GGA) with the Perdew-Burke-Ernzerhof (PBE) functional was employed in a uniform manner for all crystal structures, with the aim of further investigating the computational

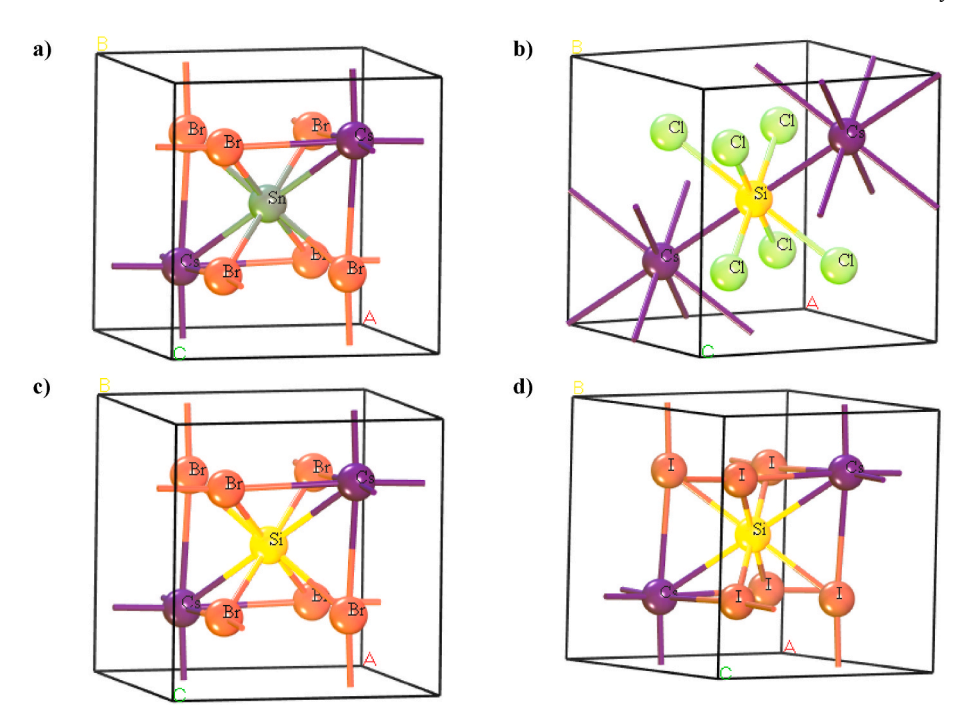


Fig. 1. a) Optimized structure of Cs<sub>2</sub>SnBr<sub>6</sub>, b)Optimized structure of Cs<sub>2</sub>SiGl<sub>6</sub>, c) Optimized structure of Cs<sub>2</sub>SiBr<sub>6</sub>and c) Optimized structure of Cs<sub>2</sub>SiI<sub>6</sub>.

determination of the band gap.

### 3. Results and discussion

### 3.1. Optimized structure and lattice parameters

After the simulation, the stable structure of Cs<sub>2</sub>SnBr<sub>6</sub> crystallizes in the cubic F  $\overline{m}$ 3 m space group. Moreover, the Cs<sup>1+</sup> is bonded to six equivalent X<sup>1-</sup> atoms to form CsBr<sub>6</sub>shown in Fig. 1 with cubic-octahedra shape. The a, b and c are 10.67 Å, 10.67 Å and 10.67 Å which are fixed for all crystals. All Cs–Br bond lengths are 4.27 Å. Sn<sup>4+</sup> is bonded to six equivalent I1- atoms to form SnI<sub>6</sub> octahedra that share faces. All Sn-Br bond lengths are 2.91 Å. Br1- is bonded in a distorted single-bond geometry to four equivalent Cs1+ and one Si4+ atom. The Cs-site atoms are located at the 8c Wyckof site and in the fractional coordinates (3/4, 3/4, 1/4), the Sn-site cations are at the 4a Wyckof site with the fractional coordinates (0, 0, 0). Lastly, the X-anions are at the 24e Wyckof site with the fractional coordinates (0.755, 1/2, 1/2). The values of the lattice parameters for Cs<sub>2</sub>SnBr<sub>6</sub>, Cs<sub>2</sub>SiCl<sub>6</sub>, Cs<sub>2</sub>SiBr<sub>6</sub> and Cs<sub>2</sub>SiI<sub>6</sub> were determined from the studio of the materials after optimizing their crystal structures, which had been listed in Table 1 as the basic structural unit, through the four methods and trying to maintain its similar parameters getting a comparative study at a point. In addition, it is noteworthy to highlight that the structural optimization depicted in Fig. 1(a)-(d) was conducted using the Generalized Gradient Approximation (GGA) with the Perdew-Burke-Ernzerhof (PBE) functional. This optimization specifically focused on investigating the electronic structure and optical properties of a crystal composed of heavy metal atoms. The usual role of density functional theory (DFT) was considered to be as such.

Investigating the relationship between the band gap, DOS, and

stability of these compounds is crucial for designing durable and commercially viable solar cells. Additionally, understanding the toxicity of these compounds is important for their safe use in photovoltaic applications.

# 3.2. Electronic band structure

The band gap or energy gap of semiconductors is a term usually used to describe the energy difference between the high-energy conduction band (CB) and the low-energy valence band (VB). This region represents a range of energy levels that are prohibited or disallowed. The presence of a substantial difference in energy levels between the conduction band (CB) and valence band (VB) is commonly acknowledged to hinder and disturb the movement of electrons following the absorption of solar radiation. This study employed the GGA with PBE functional as the initial screening method for determining the structure and structural geometry of Cs<sub>2</sub>SiBr<sub>6</sub>. The band gap of 2.434 eV was subsequently determined using this approach. Additionally, it is observed that the band gap of the generalized gradient approximation (GGA) with Perdew-Burke-Ernzerhof (PBE) functional coincided with the reference value of 2.450 eV for Cs2SnBr6. If the band gap of inorganic Pb-free perovskite solar materials falls within the range of 0.9-1.6 eV, it is possible for them to achieve an efficiency above 25 %. [18]. However, the band gap in this study of Cs<sub>2</sub>SiCl<sub>6</sub>, Cs<sub>2</sub>SiBr<sub>6</sub>, and Cs<sub>2</sub>SiI<sub>6</sub> is stayed in 1.540 eV, 1.291 eV, and 0.261 eV, respectively by GGA with PBE which is to maintain the reference of 25 % efficiency but the main crystal of Cs<sub>2</sub>SnBr<sub>6</sub> is not satisfied the band gap range in targeting 25 % efficiency. Fig. 2(b)-2(t) show the calculated band structures for A2BX6 and each figure represents the band structure of a fixed A-site cation in the Brillouin zone along the high symmetrical direction, highlighting a

Table 1 Structural calculation by four methods of Cs<sub>2</sub>SnBr<sub>6</sub>, Cs<sub>2</sub>SiCl<sub>6</sub>, Cs<sub>2</sub>SiBr<sub>6</sub> and Cs<sub>2</sub>SiI<sub>6</sub>.

Compounds	a	b	c	α	β	γ	Crystal type	Space group	Density
Cs <sub>2</sub> SnBr <sub>6</sub>	10.67 Å	10.67 Å	10.67 Å	90.00°	90.00°	90.00°	Cubic	Fm3 <del>m</del>	3.27 g cm <sup>-3</sup>
Cs <sub>2</sub> SiCl <sub>6</sub>	10.67 Å	10.67 Å	10.67 Å	$90.00^{\circ}$	$90.00^{\circ}$	$90.00^{\circ}$	Cubic	Fm3 <del>m</del>	3.27 g cm <sup>-3</sup>
Cs <sub>2</sub> SiBr <sub>6</sub>	10.67 Å	10.67 Å	10.67 Å	90.00°	90.00°	90.00°	Cubic	Fm3 <del>m</del>	3.27 g cm <sup>-3</sup>
Cs <sub>2</sub> SiI <sub>6</sub>	10.67 Å	10.67 Å	10.67 Å	90.00°	90.00°	90.00°	Cubic	Fm3 <del>m</del>	3.27 g cm <sup>-3</sup>

semiconducting property. Next, the  $Cs_2SiCl_6$ ,  $Cs_2SiBr_6$ , and  $Cs_2SiI_6$ are shown as the direct band gap materials. Furthermore, the Fig. 2(b)-2(t) demonstrate that the substitution of Cl with Br and the fixed presence of B in X site cations result in a decrease in the band gap. Although the PBE-GGA method predicts the  $Cs_2SiCl_6$ ,  $Cs_2SiBr_6$ , and  $Cs_2SiI_6$  crystals are as a semiconductor and both predicted crystals have narrow band gap semiconductor properties [19–23]. This series of compounds' k-path is W-L-G-X-Z-K. The application of OTFG Ultra soft, OTFG norm conserving, Ultra soft, and Norm conserving pseudopotential methods is of paramount importance in elucidating the electronic structure of crystals being studied.

As OTFG Ultra soft, OTFG norm conserving, ultra soft, and Norm conserving of pseudopotential methods conveys the significance role for determination of the electronic structure of studied crystals, the Table 2.

On the other hand, the second main finding of this study relates to the comparative examination of five density functional theory (DFT) functionals using the generalized gradient approximation (GGA) methodology. This analysis is presented in Table 3 and employs the norm-conserving pseudopotential technique. First of all, the GGA with PBE is found to have the almost same value of experimental data for  $\text{Cs}_2\text{SnBr}_6$  (Mother Crystal) as a result it is referenced as the more adequate method for calculating the electronic structure. In addition, according to the basis of the band gap study, the  $\text{Cs}_2\text{SiBr}_6$  may show the maximum solar efficiency in perovskite.

The band gap of a semiconductor affects its ability to absorb light and generate photoexcited carriers.  $Cs_2SiCl_6$ ,  $Cs_2SiBr_6$ , and  $Cs_2SiI_6$  exhibit different band gap values due to the variation in halogen atoms (Cl, Br, I). This allows for the tuning of the material's absorption properties to match specific regions of the solar spectrum, potentially enhancing solar cell efficiency.

By exploring compounds with different halogen atoms, the band gap can be tuned across a wide range. This versatility enables the design of multi-junction or tandem solar cell configurations that can capture a broader spectrum of sunlight, potentially improving overall efficiency.

## 3.3. Density of states (DOS) and partial density of states (PDOS)

The analysis of the density of states (DOS) and partial density of states (PDOS) offers significant insights into the electrical characteristics of a given system, encompassing the influence of orbitals and spin. The provided illustrations serve to elucidate the role of electrons in the development of electronic band structures and can be employed as a means of comprehending the phenomenon of orbital splitting [25–28]. The concept of the Total Density of States (TDOS) pertains to the comprehensive characterization of the distribution of electronic states over various energy levels inside a given system. The total density of states (TDOS) in Cs2SnBr6, Cs2SiCl6, Cs2SiBr6, and Cs2SiI6 crystals is determined by the contributions of the constituent elements found inside these crystals, namely cesium (Cs), silicon (Si), tin (Sn), chlorine (Cl), bromine (Br), and iodine (I). The visualization and characterization of the Total Density of States (TDOS) can be achieved through the utilization of a plot, such as Fig. 3(a)-(f) and Fig. S1(a)-S1(k). This plot effectively illustrates the distribution of electronic states in relation to energy.

In general, the DOS is a concept used in solid-state physics to describe the distribution of energy levels available to electrons within a material. It plays a crucial role in understanding the electronic properties and behavior of materials, including semiconductors used in solar cells. Perovskite solar cells, such as those based on  $Cs_2SiX_6$  compounds (where X represents a halogen atom: Cl, Br, I), have gained significant attention due to their potential for high-efficiency photovoltaic applications.

The DOS of a material depends on its electronic band structure, which describes the allowed energy levels and the corresponding electron states. However, providing specific density of state plots for these  $Cs_2SiX_6$  compounds is not possible without detailed electronic structure

calculations using methods like density functional theory (DFT) or other quantum mechanical techniques.

Generally, the DOS of a semiconductor like these perovskite compounds will show a continuum of energy states, separated by energy band gaps. The band gap is the energy range that electrons cannot occupy unless they gain enough energy to transition from the valence band (lower energy states) to the conduction band (higher energy states). The presence and size of this band gap significantly affect a material's electrical and optical properties.

Perovskite solar cells have been researched extensively, and their DOS and electronic properties can vary based on factors such as the specific chemical composition, crystal structure, and defects present in the material. In these compounds,  $Cs_2SiX_6$ , the Cs represents cesium ions, Si represents silicon ions, and X represents halogen ions (Cl, Br, I). The choice of halogen can affect the band gap and other electronic properties.

Fig. 3(a), which compares the DOS of  $Cs_2SnBr_6$ ,  $Cs_2SiCl_6$ ,  $Cs_2SiBr_6$ , and  $Cs_2SiI_6$  crystals, shows that  $Cs_2SiI_6$ confirms having a higher valance band electron density than  $Cs_2SnBr_6$ ,  $Cs_2SiCl_6$  and  $Cs_2SiBr_6$ . The illustration of the PDOS for  $Cs_2SnBr_6$ ,  $Cs_2SiCl_6$ ,  $Cs_2SiBr_6$ , and  $Cs_2SiI_6$  can be found in Fig. 3(b–f) and Fig S1 (a-k), the nature of the elements6s<sup>1</sup>, and  $5p^6$  for  $Cs_2SiS^2$  and  $2p^6$  for  $Si_2S^2$   $Sp^2$  and  $4d^{10}$  for  $Si_2S^2$  and  $3p^5$  for  $Cl_2As^2$   $4p^5$  and  $3d^{10}$  for  $Si_2S^2$ ,  $5p^5$  and  $4d^{10}$  for I, has been explored to help the explanation how electrons undergo hybridization and transition from the maximum valence band (MCB) to the minimum conduction band (MCB) as seen in the simulation of the DOS.

The electronic band structure, as well as the density of states (DOS) and partial density of states (PDOS), exhibit a clear correlation with chemical reactivity descriptors. The aforementioned characteristics encompass the highest occupied molecular orbital (HOMO), the lowest unoccupied molecular orbital (LUMO), and the HOMO-LUMO gap. The highest occupied molecular orbital (HOMO) is indicative of the energy level that accommodates electrons inside a given system, whereas the lowest unoccupied molecular orbital (LUMO) signifies the energy level that remains vacant. The HOMO-LUMO gap is defined as the disparity in energy levels between the highest occupied molecular orbital (HOMO) and the lowest unoccupied molecular orbital (LUMO). The aforementioned descriptors play a crucial role in ascertaining the reactivity and electronic characteristics of a given substance or molecule. Through analysis of the Density of States (DOS) and Projected Density of States (PDOS) diagrams, it is possible to discern the energy levels associated with the Highest Occupied Molecular Orbital (HOMO) and Lowest Unoccupied Molecular Orbital (LUMO). The highest occupied molecular orbital (HOMO) is observed as a discernible peak in the density of states (DOS), whereas the lowest unoccupied molecular orbital (LUMO) is typically observed as either the subsequent highest peak or as the onset of a band. The energy difference between the HOMO and LUMO levels can be used to ascertain the HOMO-LUMO gap. The HOMO and LUMO energy levels, as well as the HOMO-LUMO energy gap, are significant indicators of the chemical reactivity and electrical characteristics of a given system. These phenomena exert an impact on various processes, including electron transfer, light absorption and emission, and chemical reactions.

Determining whether a material is p-type or n-type based solely on its density of states (DOS) can be challenging because it depends on the distribution of energy levels within the valence and conduction bands. P-type and n-type behavior in semiconductors is primarily determined by the majority carrier type (holes or electrons) and the presence of acceptor or donor states, which are related to the position of the Fermi level relative to the energy bands. In a p-type semiconductor, the Fermi level (E\_F) is situated closer to the valence band (VB) than to the conduction band (CB). This means that there is an abundance of holes (positively charged carriers) in the material due to the presence of acceptor states that are relatively close to the valence band. Acceptors create energy levels within the band gap that can trap electrons, leaving behind holes. This results in a DOS that has a higher density of states

Md.H. Ali et al. Hybrid Advances 4 (2023) 100084

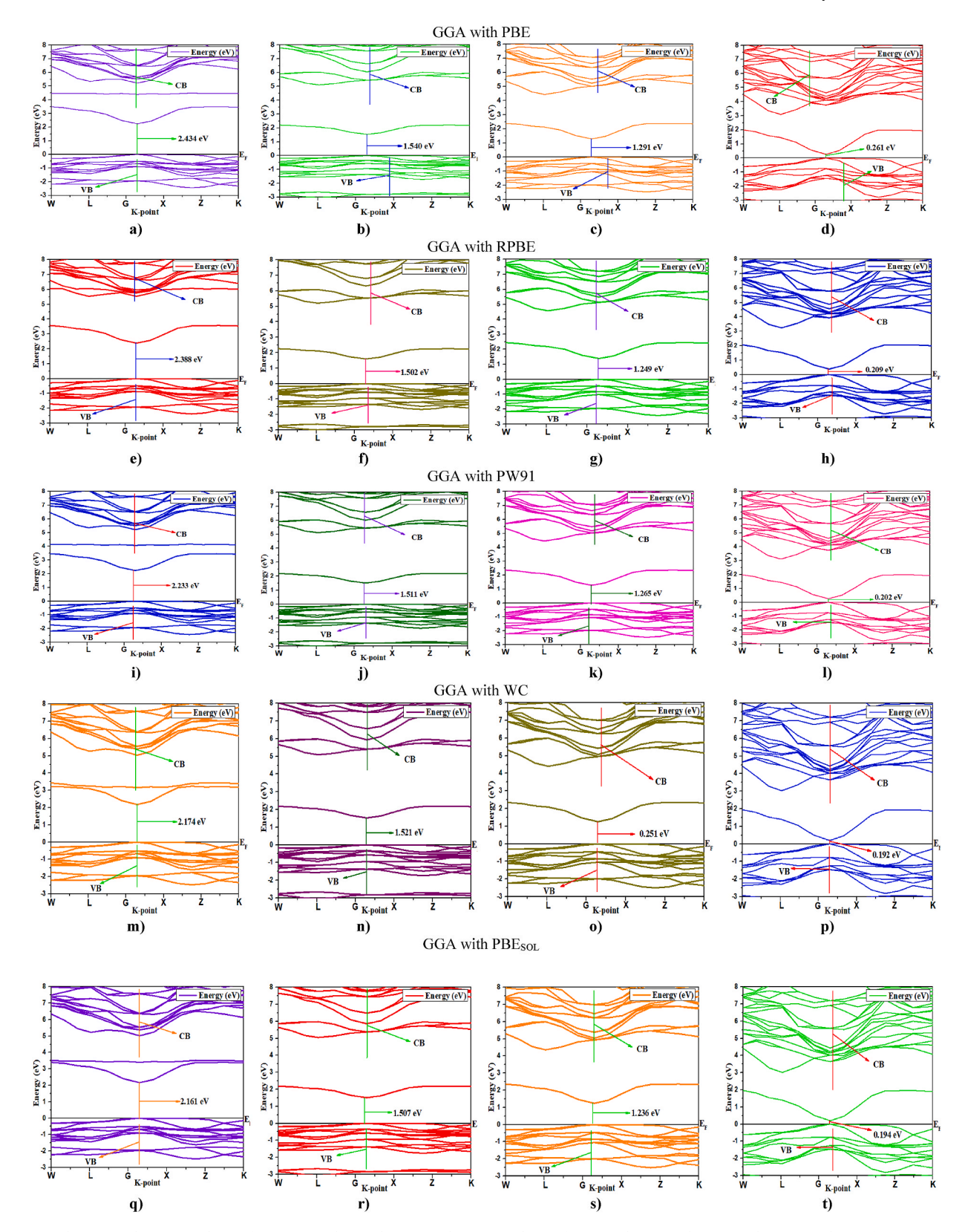


Fig. 2. a) Band structure by GGA with PBE for Cs<sub>2</sub>SiBr<sub>6</sub>, b) Band structure by GGA with PBE for Cs<sub>2</sub>SiCl<sub>6</sub>, c) Band structure by GGA with PBE for Cs<sub>2</sub>SiBr<sub>6</sub>, d) Band structure by GGA with PBE for Cs<sub>2</sub>SiI<sub>6</sub>, e) Band structure by GGA with RPBE for Cs<sub>2</sub>SiBr<sub>6</sub>, f) Band structure by GGA with RPBE for Cs<sub>2</sub>SiBr<sub>6</sub>, g) Band structure by GGA with PW91 for Cs<sub>2</sub>SiBr<sub>6</sub>, h) Band structure by GGA with PW91 for Cs<sub>2</sub>SiBr<sub>6</sub>, h) Band structure by GGA with PW91 for Cs<sub>2</sub>SiBr<sub>6</sub>, h) Band structure by GGA with PW91 for Cs<sub>2</sub>SiBr<sub>6</sub>, n) Band structure by GGA with WC for Cs<sub>2</sub>SiBr<sub>6</sub>, n) Band structure by GGA with WC for Cs<sub>2</sub>SiBr<sub>6</sub>, n) Band structure by GGA with WC for Cs<sub>2</sub>SiBr<sub>6</sub>, p) Band structure by GGA with WC for Cs<sub>2</sub>SiBr<sub>6</sub>, p) Band structure by GGA with PBE<sub>SOL</sub> for Cs<sub>2</sub>SiBr<sub>6</sub>, p) Band structure by GGA with PBE<sub>SOL</sub> for Cs<sub>2</sub>SiBr<sub>6</sub> and t) Band structure by GGA with PBE<sub>SOL</sub> for Cs<sub>2</sub>SiI<sub>6</sub>.

Table 2
Band gap by four pseudopotential methods, eV.

Crystals	OTFG Ultra soft		OTFG norm conserving		Ultra soft		Norm conserving	
	GGA with PBE	LDA with CA-PZ	GGA with PBE	LDA with CA-PZ	GGA with PBE	LDA with CA-PZ	GGA with PBE	LDA with CA-PZ
Cs <sub>2</sub> SnBr <sub>6</sub> (Mother Crystal)	2.227	2.315	2.110	1.911	2.169	1.973	2.434	2.326
Cs <sub>2</sub> SiCl <sub>6</sub>	1.468	1.397	1.339	1.402	1.401	1.436	1. 540	1.437
Cs <sub>2</sub> SiBr <sub>6</sub>	1.231	1.144	1.296	1.171	1.227	1.145	1.291	1.256
Cs <sub>2</sub> SiI <sub>6</sub>	0.207	0.116	0.212	0.105	0.201	0.128	0.216	0.182

**Table 3**Band gap with respect to various functional of crystals, eV.

	_			-		
Crystals	GGA with PBE	GGA with RPBE	GGA with PW91	GGA with WC	GGA with PBE <sub>SOL</sub>	Reference
Cs <sub>2</sub> SnBr <sub>6</sub>	2.434	2.388	2.233	2.174	2.161	2.450 eV [24]
Cs <sub>2</sub> SiCl <sub>6</sub>	1. 540	1.502	1.511	1.521	1.507	Newly Predicted
$Cs_2SiBr_6$	1.291	1.249	1.265	1.251	1.236	Newly Predicted
Cs <sub>2</sub> SiI <sub>6</sub>	0.216	0.209	0.202	0.192	0.194	Newly Predicted

near the valence band. In an n-type semiconductor, the Fermi level is positioned closer to the conduction band than to the valence band. This indicates that there are an abundance of electrons (negatively charged carriers) in the material due to the presence of donor states. Donors create energy levels within the band gap that can provide extra electrons to the conduction band. From the Fig. 3(a), it is found the DOS of Cs<sub>2</sub>SnBr<sub>6</sub>, Cs<sub>2</sub>SiCl<sub>6</sub>, Cs<sub>2</sub>SiBr<sub>6</sub>, and Cs<sub>2</sub>SiI<sub>6</sub>, so, they are p-type materials. P-type materials play a crucial role in the construction of solar cells and other semiconductor devices, including perovskite solar cells like those based on  $Cs_2SiX_6$  compounds (where X = Cl, Br, I). In a solar cell, a p-n junction is formed between the p-type and n-type materials. The p-n junction facilitates the separation of photo-generated electron-hole pairs. P-type materials are used to form the other half of this junction, allowing efficient charge separation and current generation. It's important to note that the choice of p-type material and its properties, such as its energy levels, carrier mobility, and stability, greatly influence the overall performance of the perovskite solar cell. Different compounds like Cs<sub>2</sub>SiX<sub>6</sub> (X = Cl, Br, I) might exhibit different behavior based on the specific p-type material used. Therefore, careful selection and optimization of the p-type material are essential for achieving highefficiency perovskite solar cells.

The density of states (DOS) is closely linked to electronic transport and charge recombination in a solar cell. Understanding and engineering the DOS in Cs<sub>2</sub>SnBr<sub>6</sub>, Cs<sub>2</sub>SiCl<sub>6</sub>, Cs<sub>2</sub>SiBr<sub>6</sub> can lead to improved charge carrier mobility, reduced recombination, and enhanced device performance. Moreover, they are specific p-type material.

# 3.4. Photovoltaic application

The electrical potential difference of an electric device is related to open circuit voltage ( $V_{oc}$ ) which completely depends on terms of HOMO and LUMO for the organic solar cell [29].Moreover, the energy expended during the generation of the photo charge is attributed to the energy difference between the valence and conduction bands, or alternatively, the discrepancy between the highest occupied molecular orbital and lowest empty molecular orbital. The effectiveness of charge transfer between the donor and acceptor relies on the energy levels of the highest occupied molecular orbital (HOMO) and lowest unoccupied molecular orbital (LUMO) of both the donor and acceptor components. The open circuit voltage (Voc) of a solar cell is influenced by the energy dissipation that occurs during the generation of photo charge. This dissipation

is determined by the difference in energy levels between the highest occupied molecular orbital (HOMO) of the donor electrons and the lowest unoccupied molecular orbital (LUMO) of the acceptor electrons [30]. The  $V_{oc}$  parameter is determined by the formula below [31]. Voc = EHOMO(D) - ELUMO(A) - 0.3.

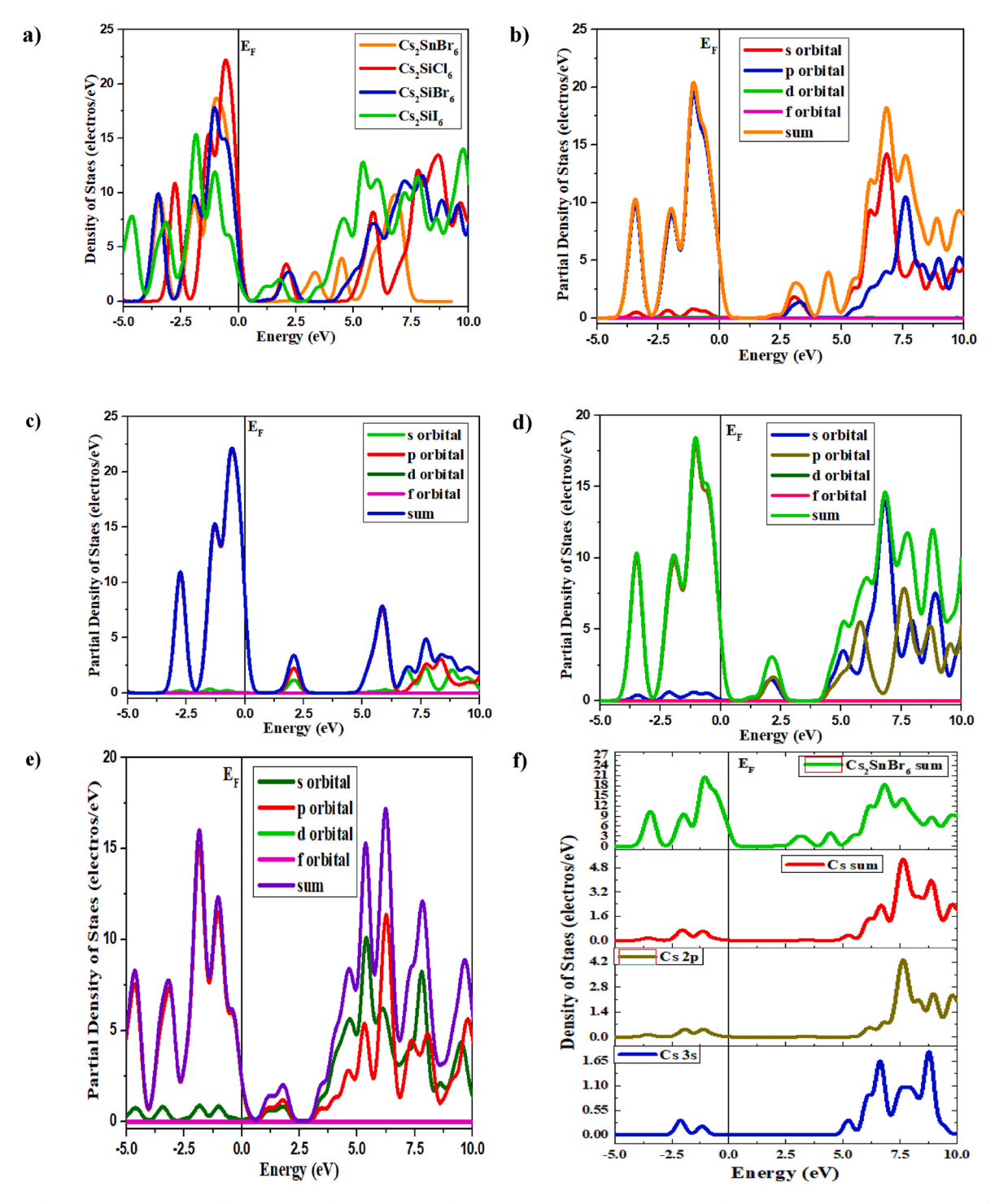
The LUMO-HOMO gap of the most chemically and physically stable organic compound is commonly observed to fall within the range of 4.0–9.0 electron volts (eV). [32,33].Furthermore, a larger energy gap serves as an indication of enhanced chemical reactivity and heightened physical stability. Within the framework of HOMO, the presence of a green hue indicates the positive node, whereas the navy-blue hue represents the negative node of the orbital. In the case of LUMO, cyan color is positive and deep orange is negative shown in Fig. 4 and Fig. 2.The current study presents the LUMO-HOMO gap values of crystals, which are listed in Table 4 as 3.318 eV, 8.753 eV, 8.098 eV, and 6.718 eV, respectively. However, the  $V_{\rm oc}$  is found at 3.018, 8.453, 7.798 and 6.718 for  $Cs_2SnBr_6$ ,  $Cs_2SiCl_6$ ,  $Cs_2SiBr_6$ , and  $Cs_2Sil_6$  crystals, respectively where the  $Cs_2SiCl_6$  maintains the maximum value of  $V_{\rm oc}$ .

### 3.5. Optical properties

The implementation of solids is significantly impacted by a range of parameters, including band structure, excitations, impurity levels, localized defects, and lattice vibrations. In addition, it is crucial to examine optical parameters such as absorption, refractive index, dielectric function  $\varepsilon(\omega)$ , optical conductivity, and loss function [34]. The primary characteristic associated with the reflectivity of a surface is its ability to reflect radiant energy. This term pertains to a specific portion of electromagnetic radiation that experiences reflection when it encounters a boundary, which is commonly referred to as the incident wave. The phenomenon of reflectance can be understood as the response of a material's electrical structure to an electromagnetic field generated by light. The aforementioned property typically relies on the characteristics of the light, including its frequency or wavelength, polarization, and angle of incidence. Several previous research studies have provided evidence that reduced reflectivity is a reliable indicator of increased absorption of ultraviolet (UV) or visible light [35-39]. Fig. 5 shows the reflectivity of Cs<sub>2</sub>SnBr<sub>6</sub>, Cs<sub>2</sub>SiCl<sub>6</sub>, Cs<sub>2</sub>SiBr<sub>6</sub>, and Cs<sub>2</sub>SiI<sub>6</sub> at energies ranging from 0.0 to 5.0 eV. Initially, Cs<sub>2</sub>SiI<sub>6</sub> had a reflectivity of about 0.45, while Cs<sub>2</sub>SiCl<sub>6</sub> and Cs<sub>2</sub>SiBr<sub>6</sub> had reflectivity of 0.35 and 0.25, respectively. The reflectivity of Cs<sub>2</sub>SnBr<sub>6</sub> increased gradually with increasing photon energy to reach 0.32, whereas the reflectivity of Cs<sub>2</sub>SiCl<sub>6</sub>, Cs<sub>2</sub>SiBr<sub>6</sub>, and Cs<sub>2</sub>SiI<sub>6</sub> decreased until energy 2.5 eV.

Fig. 6 displays calculated absorption coefficients  $\alpha$  ( $\omega$ ) for crystals of Cs<sub>2</sub>SnBr<sub>6</sub>, Cs<sub>2</sub>SiCl<sub>6</sub>, Cs<sub>2</sub>SiBr<sub>6</sub>, and Cs<sub>2</sub>SiI<sub>6</sub> with absorption edges at 0.2–2.5 eV that are reasonably in agreement with the corresponding band gap. The absorption peaks that have a positive correlation are ascribed to the electronic transitions that take place between bonding and anti-bonding states [40]. The maximum absorption spectra of Cs<sub>2</sub>SiCl<sub>6</sub>, Cs<sub>2</sub>SiBr<sub>6</sub>, and Cs<sub>2</sub>SiI<sub>6</sub>are higher than Cs<sub>2</sub>SnBr<sub>6</sub> in the visible energy range. As a result, the Si atom is a viable alternative to Sn atom in inorganic perovskite solar cells. The maximum of the absorption peaks within this group (Cs<sub>2</sub>SiX<sub>6</sub>) significantly decreases as photon energy raises as a result of increasing halogen radii. The leftover compounds demonstrate ultraviolet peaks that are suitable for utilization in optical

Md.H. Ali et al. Hybrid Advances 4 (2023) 100084



 $\label{eq:Fig. 3. a) Total DOS for $Cs_2SnBr_6$, $Cs_2SiCl_6$, $Cs_2SiCl_6$, $Cs_2SiBr_6$, and $Cs_2Sil_6$, $b$) Partial Density of States for $Cs_2SnBr_6$, $c$) Partial Density of States for $Cs_2SiBr_6$, $c$) Partial Density of S$ 

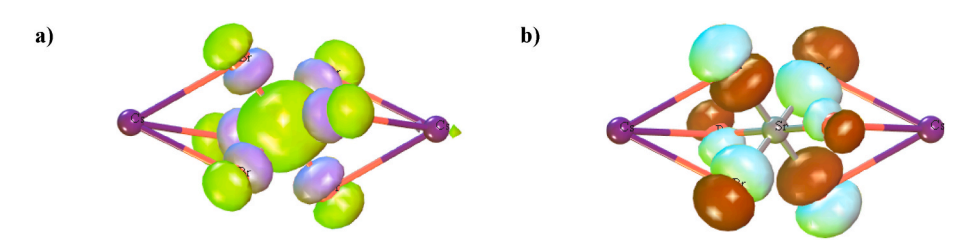


Fig. 4. a) LUMO for Cs<sub>2</sub>SnBr<sub>6</sub>, b) HOMO for Cs<sub>2</sub>SnBr<sub>6</sub>.

Table 4
Data of HOMO, LUMO Open circuit voltage.

	$Cs_2SnBr_6$	$Cs_2SiCl_6$	$Cs_2SiBr_6$	$Cs_2SiI_6$	Formula
LUMO, eV HOMO, eV \( \Delta \) E, (LUMO- HOMO) gap	-3.623 -6.941 3.318	-0.587 -9.340 8.753	-0.546 -8.644 8.098	-0.771 -7.489 6.718	$\begin{split} E_{gap} &= (\; E_{LUMO} \; - \\ E_{HOMO}) \approx IP - EA \end{split}$
Open circuit voltage (V <sub>oc</sub> ), eV	3.018	8.453	7.798	6.718	Voc = EHOMO(D) - ELUMO(A) - 0.3

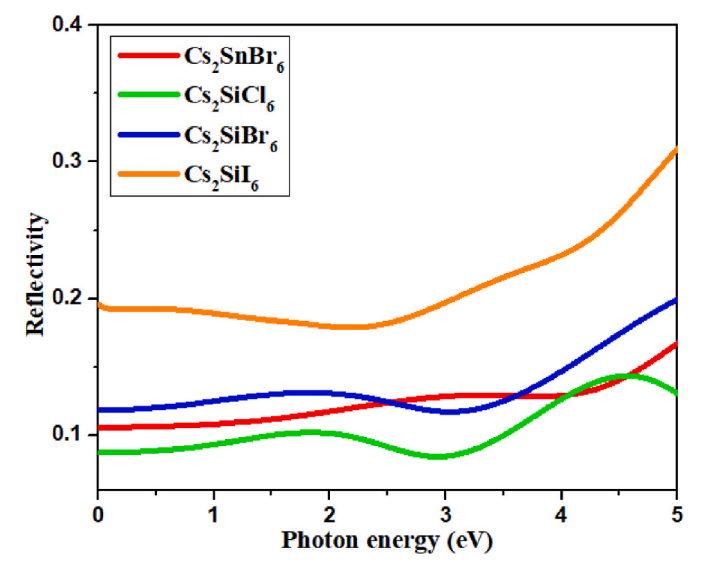


Fig. 5. Reflectivity.

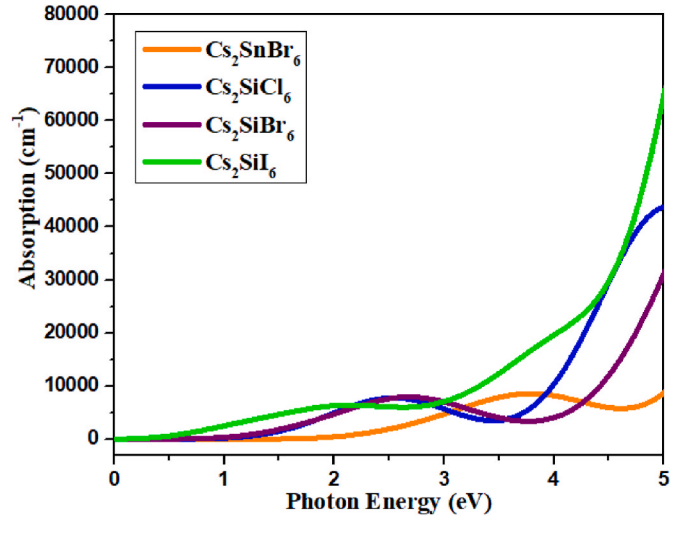


Fig. 6. Absorption.

devices operating within this specific wavelength range. The efficacy of the spectroscopic-limited maximum efficiency (SLME) criterion in assessing the photovoltaic efficiency of a solar absorber has been successfully proven [41]. This study examines various aspects including the band gap, optical absorption spectrum, recombination mechanism, and fundamental transition. Fig. 6 depicts the computed SLME for our compounds. Cs<sub>2</sub>SiCl<sub>6</sub>, Cs<sub>2</sub>SiBr<sub>6</sub>, and Cs<sub>2</sub>SiI<sub>6</sub> crystals have a higher

spectroscopic-limited maximum efficiency than the  $Cs_2SnBr_6$ , which can be attributed to their favorable band gap and optimal light absorption.

The refractive index is an essential and distinctive physical property that holds significant importance in the characterization of materials, specifically in the domain of semiconductors. The determination of a semiconductor's refractive index relies on the analysis of its band gap [42]. The growth circumstances of III-V alloy semiconductors have a substantial impact on their properties, mostly due to the presence of defects, mismatches, and impurity diffusion inside the bulk of the semiconductor [43]. The refractive index of Cs<sub>2</sub>SnBr<sub>6</sub>, Cs<sub>2</sub>SiCl<sub>6</sub>, Cs<sub>2</sub>SiBr<sub>6</sub>, and Cs<sub>2</sub>SiI<sub>6</sub> as a function of photon energy is shown in Figs. 3(a) and S3 (b). For crystals of Cs<sub>2</sub>SnBr<sub>6</sub>, Cs<sub>2</sub>SiCl<sub>6</sub>, Cs<sub>2</sub>SiBr<sub>6</sub>, and Cs<sub>2</sub>SiI<sub>6</sub>, the refractive index is at 1.9, 1.7, 2.1, and 2.6 in the infrared region (0.2 eV-1 eV), drops quickly in the visible region, and then rises once more in the ultraviolet region up to 5 eV. The refractive index demonstrates a noticeable rise within the infrared range, followed by a progressive decrease in the visible and ultraviolet ranges. A uniform reflectance value of 100 % was consistently recorded across the energy range spanning from 2.2 to 30 electron volts (eV) [44]. Consequently, the results show that Cs<sub>2</sub>SiCl<sub>6</sub>, Cs<sub>2</sub>SiBr<sub>6</sub>, and Cs<sub>2</sub>SiI<sub>6</sub> are the best reflectors and can also reduce solar heating [45]. The reflectivity refractive index spectrum of Cs<sub>2</sub>SiI<sub>6</sub> is always significantly larger than among Cs<sub>2</sub>SnBr<sub>6</sub>, Cs<sub>2</sub>SiCl<sub>6</sub>, and Cs<sub>2</sub>SiBr<sub>6</sub> crystals.

Fig. 7(a) and (b) contain real  $\varepsilon 1(\omega)$  and imaginary  $\varepsilon 2(\omega)$  parts of the dielectric function. The real part of the dielectric constant of Cs<sub>2</sub>SiI<sub>6</sub> is much greater than others, and the larger value of the dielectric constant indicates the large efficient light absorption. The observed phenomenon possesses the capability to reduce the occurrence of radioactive electronhole recombination and facilitate the maintenance of low levels of charge defects [46]. It is clear from Fig. 7(a) that the real part,  $\varepsilon 1(\omega)$  of Cs<sub>2</sub>SiCl<sub>6</sub>, Cs<sub>2</sub>SiBr<sub>6</sub> and Cs<sub>2</sub>SiI<sub>6</sub> are shifted towards the visible region by replacing the halide ions (Cl→Br→I) across the selected compounds, resulting in an increase in  $\varepsilon 1(\omega)$ , and shifting of peaks towards the low energies. In the case of the imaginary parts of the dielectric function, the threshold energies of 2.434 eV (Cs<sub>2</sub>SnBr<sub>6</sub>), 1.540 eV (Cs<sub>2</sub>SiCl<sub>6</sub>), 1.291 eV (Cs<sub>2</sub>SiBr<sub>6</sub>), and 0.216 eV (Cs<sub>2</sub>SiI<sub>6</sub>) are found shown in Fig. 7(a) and (b). The estimated intensities of  $\varepsilon 2(\omega)$  for the compounds containing iodide exhibit a higher magnitude in comparison to the compounds containing bromide and chloride, as depicted in Fig. 7 (b). The primary factor seems to be that the band gap of the preceding phases is somewhat smaller than that of the subsequent ones. Based on the principles outlined in the Fermi golden rule, it can be observed that compounds containing bromine (Br) and chlorine (Cl) have a comparatively reduced transition

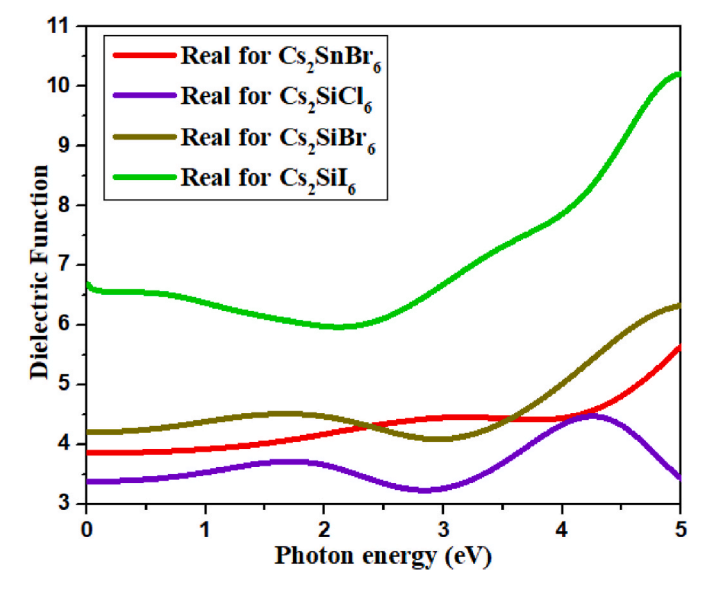


Fig. 7. a). Dielectric Function (Real part).

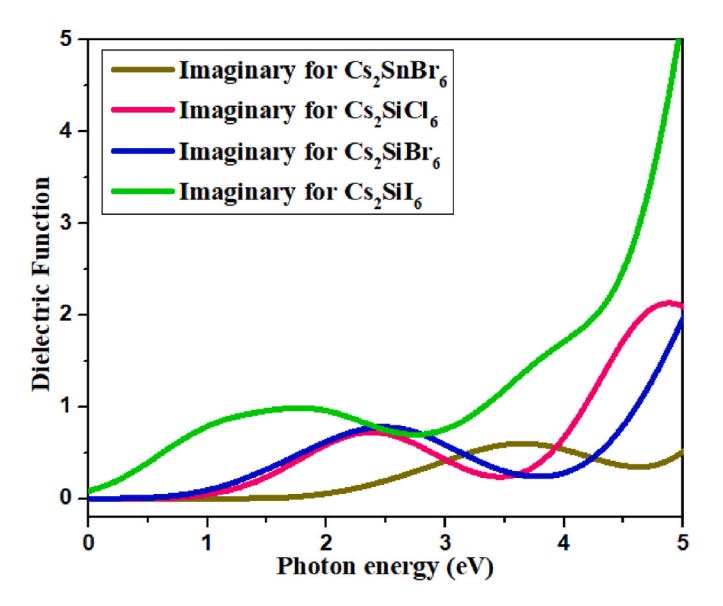


Fig. 7. b). Dielectric Function (Imaginary part).

probability [47].

The determination of conductivity and the majority of charged reactions heavily relies on the analysis of the band gap and optical frequencies associated with electrical conduction [48]. The term "electronic conduction" pertains to the ability to facilitate the movement or transfer of unbound electrons by providing the necessary energy for a transition. Furthermore, optical conductivity determines the free electron in the valance bond. The Fig. S4 depicts the conductivity spectra of Cs2SiCl6, Cs2SiBr6, and Cs2SiI6 crystals at 0.2–5.0 eV and demonstrates the semiconductor nature of Cs2SnBr6, Cs2SiCl6, Cs2SiBr6, and Cs2SiI6 crystals. From Fig. 4, it is found that the conductivity of Cs2SiI6 is achieved the largest possibility for the free electrons transition after 4.0 eV although other crystals show the similar trend having the changing of halogen.

The Fig. S5 conveys the computed energy loss spectra. In order to fully understand the excitation spectra obtained from screening, it is beneficial to have a thorough understanding of the energy loss function of materials. This information is essential since it represents a significant constraint within the dielectric formalism [49], as well as speed of electron transports in a material [50], valence inter-band transitions or electrons in the atom's outer shell [51]. Additionally, the loss function consists of two discrete photon energy areas, specifically the lower photon energy region and the higher photon energy region, which are relevant to crystal materials. The dielectric function refers to the response of a semiconductor to an external electromagnetic disturbance, as observed by the energy loss function. In comparison to Cs<sub>2</sub>SiI<sub>6</sub>, the energy loss functions of Cs<sub>2</sub>SnBr<sub>6</sub>, Cs<sub>2</sub>SiCl<sub>6</sub>, and Cs<sub>2</sub>SiBr<sub>6</sub> are all quite low in the visible energy range.

The optical properties of these crystals, such as absorption and emission spectra, can be tailored by adjusting their composition. This tuning can enable efficient light absorption and charge generation, contributing to higher power conversion efficiencies in solar cells.

### 3.6. Aquatic toxicity

The public's view and acceptance of perovskite solar cells are impeded by apprehensions over their toxicity, primarily attributed to the inclusion of lead. The subject matter in question has incited discussions and resistance, notwithstanding the acknowledgment of the industrial significance of CdTe solar cells, which consist of hazardous heavy metals, dating back to the 1990s. Despite apprehensions regarding their potential health and environmental ramifications [52]. The second notable issue concerns the biodegradability and instability of

crystals. The presence of great biodegradability in these crystals holds considerable promise for the reduction of environmental and health risks [53].

Aquatic toxicity refers to the investigation of the effects of both anthropogenic and natural compounds on aquatic species. These effects can have significant consequences on entire ecosystems and communities by impacting individual organisms.

The AMES toxicity of the mentioned perovskite compounds (Cs<sub>2</sub>SiX<sub>6</sub>, where X = Cl, Br, I). The AMES test is a bacterial reverse mutation assay used to assess the mutagenic potential of chemicals or compounds. Toxicity studies and assessments can change over time as new research is conducted and more data becomes available. It suggests that these compounds have exhibited mutagenic potential in the AMES test, which could indicate that they have the potential to cause genetic mutations. If these compounds have indeed shown positive results in the AMES test for mutagenicity, it raises concerns about their safety, especially in terms of potential effects on human health and the environment. Further assessment and research would be necessary to understand the extent of their toxicity, potential exposure pathways, and appropriate safety measures to mitigate their negative impacts. It is concerns for Cs<sub>2</sub>SnBr<sub>6</sub> but not applicable for Cs<sub>2</sub>SnCl<sub>6</sub> and Cs<sub>2</sub>SnI<sub>6</sub> due to having no AMES toxicity. Secondly, all of newly designed crystals are not carcinogenic but parent crystal of lead (Cs<sub>2</sub>PbBr<sub>6</sub>) can show carcinogenetic character even not found the inhibition character show in Table 5.

(Cs<sub>2</sub>SiX<sub>6</sub>, where X = Cl, Br, I) are inorganic compounds, and in general, inorganic compounds tend to have low or no biodegradability. This means that they are not easily broken down by natural biological processes, unlike organic compounds that contain carbon-carbon or carbon-hydrogen bonds which are typically more susceptible to biodegradation. As a result, (Cs<sub>2</sub>SiX<sub>6</sub>, where X = Cl, Br, I) might exhibit toxicity to various organisms, including aquatic life, plants, and potentially humans, depending on the specific compound and its properties.

Water solubility is an important property that affects how a chemical compound interacts with water and its potential for dispersion in the environment. The water solubility value of a compound can influence its transport, distribution, and potential impact. For compounds like  $s_2SiCl_6$ ,  $Cs_2SiBr_6$ , and  $Cs_2SiI_6$ , which are inorganic compounds, their water solubility values can have various environmental impacts. It's important to note that the specific impacts depend on the water solubility value, the toxicological properties of the compounds, their concentrations in the environment, and the characteristics of the ecosystems they interact with. To fully assess the potential impacts of  $s_2SiCl_6$ ,  $Cs_2SiBr_6$ , and  $Cs_2SiI_6$ , additional information about their water solubility values and toxicological profiles would be needed.

Investigating the relationship between the band gap, DOS, and stability of these compounds is crucial for designing durable and commercially viable solar cells. Additionally, understanding the toxicity of these compounds is important for their safe use in photovoltaic applications.

# 4. Conclusion

In this study, using the same condition, the GGA with PBE, GGA with RPBE, GGA with PW9, GGA with WC, and GGA with PBE $_{SOL}$  methods have been employed using first principles of DFT to calculate the electronic structure and electronic band gap of perovskites  $A_2BX_6$  (A=Cs, B=Si; and X=Cl, Br, and I). Among the several approaches considered, the GGA with PBE method was found to be the most accurate for electrical structure calculations, as it closely matched the experimental data on band gap. Additionally, the GGA with RPBE method exhibited a similar level of accuracy to the GGA with PBE method. Secondly, the calculated electronic structure of  $A_2BX_6$  family is a narrow band gap contained  $Cs_2SiCl_6$ ,  $Cs_2SiBr_6$ , and  $Cs_2SiI_6$  crystals. The band gap was obtained in the optimal range of 0.9-1.6 eV only for  $Cs_2SiCl_6$  (1.540 eV),  $Cs_2SiBr_6$  (1.291 eV), and  $Cs_2SiI_6$  (0.216 eV) among the entire group of compounds studied. Thirdly, an alternative method for the Local Density

**Table 5** Aquatic and non -aquatic toxicity.

Crystal	AMES toxicity	Inhibition	Carcinogenicity	Water solubility, Log S	Acute Oral Toxicity, kg/mol	Oral Rat Acute Toxicity (LD50) (mol/ kg)	Honeybee Toxicity	Fish Toxicity pLC50 mg/ L	T.Pyriformis toxicity (log μg/L)	Biodegradation
Cs <sub>2</sub> PbBr <sub>6</sub>	Yes (high)	No	Yes	-3.368	0.490	2.781	High	1.417 High	1.228 High	Not readily biodegradable
Cs <sub>2</sub> SnBr <sub>6</sub>	Yes (slightly	No	No	-4.532	0.473	2.751	High	0.8185 High	1.128 High	Not readily biodegradable
Cs <sub>2</sub> SiCl <sub>6</sub>	No	No	No	-4.757	0.388	3.006	low	0.8616 High	0.954 High	Not readily biodegradable
$Cs_2SiBr_6$	Yes (slightly	No	No	-4.464	0.473	2.751	High	0.818 High	1.128 (High)	Not readily biodegradable
Cs <sub>2</sub> SiI <sub>6</sub>	No	No	No	-3.417	0.440	2.821	low	0.767 low	0.845 low	Not readily biodegradable

Approximation (LDA) demonstrates notable differences in the calculation of electronic structure for the crystals being studied, suggesting that the Generalized Gradient Approximation (GGA) is somewhat more accurate than LDA methods. In general, a significant association is observed between the ideal band gap and the attainment of high solar efficiency. Materials that demonstrate a high level of solar effectiveness have the potential to be utilized in single-junction solar cells. All the crystals stay in the band gap region of more than 25 % solar efficacy which is more verified by the calculation of open circuit voltage (Voc). In the case of V<sub>oc</sub>, the value of crystals (Cs<sub>2</sub>SnBr<sub>6</sub>, Cs<sub>2</sub>SiCl<sub>6</sub>, Cs<sub>2</sub>SiBr<sub>6</sub>, and Cs<sub>2</sub>SiI<sub>6</sub>) is in 3.018, 8.453, 7.798 and 6.718 eV, respectively. However, the Voc indicates the better efficiency for all crystals where Cs<sub>2</sub>SiCl<sub>6</sub> shows the highest value. Moreover, it is likely that the differences in electronegativity or atomic size among the atoms present in the X-sites are accountable for the observed discrepancies in the band gap. It has been shown that there is a negative correlation between the atomic size of halides and the band gap, wherein an increase in atomic size leads to a decrease in the band gap. Based on computer research, it has been observed that an increase in the atomic size of halide ions can lead to a corresponding enhancement in solar efficiency. Furthermore, we conducted calculations on the optical properties of these substances, such as reflectance, absorption, refractive index, complex dielectric function, conductivity, and loss function, in order to provide evidence for their potential applicability in various optoelectronic applications. In conclusion, the newly developed crystals demonstrate an absence of carcinogenic activity, while the crystals containing lead do not possess this characteristic. In addition, these substances demonstrate a low level of AMES toxicity and possess favorable solubility characteristics. In summary, it can be asserted that these materials do not possess inherent stability and may not easily undergo biodegradation, thereby presenting a possible environmental risk due to their ability to disperse widely. However, investigating the environmental impact of these compounds, considering factors like toxicity and long-term stability, is crucial for their practical use in solar cell technologies.

### **Funding**

The authors declare that no funds or grants were received from any institutions for this research.

# Data availability enquiries about data

Availability should be directed to the authors.

# Declaration of competing interest

On behalf of all the authors, I declare that they have no known competing financial interests or personal relationships that could have appeared to influence the work reported in this paper.

## Appendix A. Supplementary data

Supplementary data to this article can be found online at https://doi.org/10.1016/j.hybadv.2023.100084.

### References

- [1] S.-L.X. Yao, Hui Zheng, Teng-Fei Liu, Sui-Jun Chen, Jing-Lin Wen, He-Rui, Rare fluorescence red-shifted metal—organic framework sensor for methylamine derived from an N-donor ligand, Cryst. Growth Des. 21 (10) (2021) 5765–5772.
- [2] T. K, J.H. L, D. M, H.R. M, Kim, Luminescent Li-based metal-organic framework tailored for the selective detection of explosive nitroaromatic compounds: direct observation of interaction sites, Inorg. Chem. 52 (2) (2013) 589–595.
- [3] W. Z. G.E. E, H.J. S, Metal halide perovskites for energy applications, Nat. Energy 1 (6) (2016) 1–8.
- [4] F. Zhang, H. Lu, J. Tong, J.J. Berry, M.C. Beard, K. Zhu, Advances in twodimensional organic–inorganic hybrid perovskites, Energy Environ. Sci. 13 (4) (2020) 1154–1186.
- [5] A.E. M, A.M. G, M.M. B, E.M. M, D.O. S, J.R. N, Defect tolerance to intolerance in the vacancy-ordered double perovskite semiconductors Cs2SnI6 and Cs2TeI6, J. Am. Chem. Soc. 138 (27) (2016) 8453–8464.
- [6] A.W. A, F.S.X. T, D.S.C. H, S. S, L.N. Ahmad, Tin and germanium substitution in lead free perovskite solar cell: current status and future trends, in: IOP Conference Series: Materials Science and Engineering, vol. 957, IOP Publishing, 2020, 012057, 1
- [7] D. Y, Y. G, Y. Z, Q. F, J. W, Y. Y, Z. Xiaozhang, Air-stable n-type thermoelectric materials enabled by organic diradicaloids, Angew. Chem. Int. Ed. 58 (15) (2019) 4958–4962.
- [8] M.-G. J, M. C, Y. Z, H.F. G, J. D, L. M, N.P. P, Z.X. Cheng, Earth-abundant nontoxic titanium (IV)-based vacancy-ordered double perovskite halides with tunable 1.0 to 1.8 eV bandgaps for photovoltaic applications, ACS Energy Lett. 3 (2) (2018) 297–304.
- [9] N.H. Sakai, Amir Abbas Filip, Marina R. Nayak, Pabitra K. Nayak, Simantini Ramadan, Alexandra Wang, Zhiping Giustino, Feliciano Snaith, J. Henry, Solution-processed cesium hexabromopalladate (IV), Cs2PdBr6, for optoelectronic applications, J. Am. Chem. Soc. 139 (17) (2017) 6030–6033.
- [10] M.-G.C. Ju, Min Zhou, Yuanyuan Garces, Hector F. Dai, Jun Ma, Padture Liang, Nitin P. Zeng, Xiao Cheng, Earth-abundant nontoxic titanium (IV)-based vacancyordered double perovskite halides with tunable 1.0 to 1.8 eV bandgaps for photovoltaic applications, ACS Energy Lett. 3 (2) (2018) 297–304.
- [11] X.-G.Y. Zhao, Dongwen Ren, Ji-Chang Sun, Yuanhui Xiao, Zewen Zhang, Lijun, Rational design of halide double perovskites for optoelectronic applications, Joule 2 (9) (2018) 1662–1673.
- [12] Y.X. Cai, Wei Ding, Hong Chen, Thirumal Yan, Krishnamoorthy Wong, Lydia H. Mathews, Nripan Mhaisalkar, Subodh G. Sherburne, Matthew Asta, Mark, Computational study of halide perovskite-derived A2BX6 inorganic compounds: chemical trends in electronic structure and structural stability, Chem. Mater. 29 (18) (2017) 7740–7749.
- [13] J. K. Islam, Ajoy Chakma, Unesco Alam, Md Biswas, Shimul Ahmad, Zubair Islam, Md Jony, Ms Ismat Jahan Ahmed, Md Boshir, "Investigation of structural, electronic, and optical properties of SrTiO3 and SrTiO. 94AgO. 06O3 quantum dots based semiconductor using first principle approach," Adv. J. Chem.-Section A, vol. 5, no. 2, pp. 164-174.
- [14] M.I. Ali, MJ, M. Rafid, R.R. Jeetu, R. Roy, U. Chakma, The computational screening of structural, electronic, and optical properties for SiC, Si<sub>0.94</sub>Sn<sub>0.06</sub>C, and Si<sub>0.88</sub>Sn<sub>0.12</sub>C lead-free photovoltaic inverters using DFT functional of first principle approach, Eurasian Chem. Commun. 3 (5) (2021) 327–338.
- [15] M.T.K. Islam, Ajoy, Unesco Chakma, Debashis Howlader, A computational investigation of electronic structure and optical properties of AlCuO<sub>2</sub> and AlCuO<sub>.</sub> 96Fe<sub>0.</sub> 04O<sub>2</sub>: a first principle approach, Orbital - Electron. J. Chem. (2021) 58–64.
- [16] U.K. Chakma, Ajoy, Kamal Bikash Chakma, Md Tawhidul Islam, Debashis Howlader, Rasha MK. Mohamed, Electronics structure and optical

- properties of SrPbO3 and SrPbO. 94FeO. 06O3: a first principle approach, Eurasian Chem. Commun. 2 (5) (2020) 573–580.
- [17] U.K. Chakma, Ajoy, Kamal Bikash Chakma, Md Islam, Debashis Howlader, Electronics structure and optical properties of Ag2BiO3,(Ag2) 0.88 Fe0. 12BiO3: a first principle approach, Adv. J. Chem.-Section A 3 (4) (2020) 542-550.
- [18] M.B. Faizan, K.C. Murtaza, Ghulam He, Kulhari Xin, Neeraj AL-Anazy, Murefah Mana Khan, Haidar Shah, Electronic and optical properties of vacancy ordered double perovskites A2BX6 (A= Rb, Cs; B= Sn, Pd, Pt; and X= Cl, Br, I): a first principles study, Sci. Rep. 11 (1) (2021) 1-9.
- [19] M.I. Ali, Mohammad Jahidul, Ajoy Kumer, Md Hossain, Unesco Chakma, Debashis Howlader, Md Islam, Tomal Hossain, Investigation of structural, electronic and optical properties of Na 2 InAgCl 6, K 2 InAgCl 6, and Rb 2 InAgCl 6 lead-free halide double perovskites regarding with Cs 2 InAgCl 6 perovskites cell and a comparative study by DFT functionals, Mater. Res. 24 (2021).
- [20] U.K. Chakma, Ajoy, Md Al Mashud, Md Hossain, Md Alam, Md Islam, Rubel Shaikh, Ismat Jahan Jony, Jahedul Islam, Investigation of electronic structure, optical properties, map of electrostatic potential, and toxicity of HfO2, Hf0. 88Si0. 12O2, Hf0. 88Ge0. 12O2 and Hf0. 88Sn0. 12O2 by computational and virtual screening, J. Comput. Electron. (2022) 1-16.
- [21] D.H. Howlader, Md Sayed, Unesco Chakma, Ajoy Kumer, Mohammad Jahidul Islam, Md Tawhidul Islam, Tomal Hossain, Jahedul Islam, Structural geometry, electronic structure, thermo-electronic and optical properties of GaCuO2 and GaCu0. 94Fe0. 06O2: a first principle approach of three DFT functionals, Mol. Simulat. 47 (17) (2021) 1411–1422.
- [22] A.M.A. Al Mamun, Md, Ahsan Habib, Unesco Chakma, Mokit Sikder, Ajoy Kumer, Structural, electronic, optical properties and molecular dynamics study of WO3 W0. 97Ag0. 03O3 and W0. 94Ag0. 06O3 photocatalyst by the first principle of DFT study, Egypt. J. Chem. 64 (9) (2021) 5117-5126.
- [23] M.M.K. Hasan, Ajoy, Unesco Chakma, Theoretical investigation of doping effect of Fe for SnWO4 in electronic structure and optical properties: DFT based first principle study, Adv. J. Chem.-Section A 3 (5) (2020) 639–644.
- [24] M.M.G. Karim, Alex M. Pieters, Laura Winnie Leung, W.W. Wade, Jessica Zhang, Lina Scanlon, David O. Palgrave, G. Robert, Anion distribution, structural distortion, and symmetry-driven optical band gap bowing in mixed halide Cs2SnX6 vacancy ordered double perovskites, Chem. Mater. 31 (22) (2019) 9430-9444.
- [25] K.A.K. Hoque, Ajoy, Unesco Chakma, Al-Nakib Chowdury, Facile synthesis of computationally designed MgAl2O4/CeO2/Cu2o and MgAl2O4/CeO2/Ag2o smart heterojunction photocatalysts for aqueous organic pollutants degradation, ECS Trans. 107 (1) (2022), 13785.
- [26] A.-N. Chowdhury, K.A. Hoque, A. Kumer, Facile synthesis of computationally designed MgAl2O4/CeO2/Cu2O and MgAl2O4/CeO2/Ag2O smart heterojunction photocatalysts for aqueous organic pollutants degradation, SPAST Abstracts 1 (2021), 01.
- [27] M.A.K. Mahmud, Ajoy, Unesco Chakma, Debashis Howlader, Khondaker Afrina Hoque, Al-Nakib Chowdury, Fabrication of computationally designed cathode material for a high-performance Na-ion battery, ECS Trans. 107 (1) (2022), 15681.
- [28] M.M.C. Sikder, Unesco, Ajoy Kumer, Mohammad Jahidul Islam, Ahsan Habib, Md Monsur Alam, The exploration of structural, electronic and optical properties for MoS2 and MoO 95W0 05S2 photocatalyst effort on wastewater treatment using DFT functional of first principle approach, Appl. J. Environ. Eng. Sci. 7 (1) (2021) 103-113, 7-1 (2021).
- [29] G. Chamberlain, Organic solar cells: a review, Sol. Cell. 8 (1) (1983) 47–83.
  [30] P.P.R. Khlyabich, Andrey E, Barry C. Thompson, Yueh-Lin Loo, Structural origins for tunable open-circuit voltage in ternary-blend organic solar cells, Adv. Funct. Mater. 25 (34) (2015) 5557-5563.
- [31] E.A.A. Aziz, Amine Mohammed, Bouachrine, DFT study of electronic and optical properties of small oligothiophenes based on terthiophene end-capped by several donor groups, Orbital - Electron, J. Chem. 9 (3) (2017) 188-196.
- [32] A.M.K. Voutchkova, Jakub Steinfeld, Justin B. Emerson, John W. Brooks, Bryan W. Anastas, Paul Zimmerman, B. Julie, Towards rational molecular design: derivation of property guidelines for reduced acute aquatic toxicity, Green Chem. 13 (9) (2011) 2373–2379.

- [33] T.H. Hossain, Md, Md Ali, Unesco Chakma, Ajoy Kumer, Mohammad Jahidul Islam, Investigation of optoelectronics, thermoelectric, structural and photovoltaic properties of CH3NH3SnBr3 lead-free organic perovskites, Chem. Method. 5 (3) (2021) 259–270.
- [34] C.G.J. Van de Walle, Anderson, Advances in electronic structure methods for defects and impurities in solids, Phys. Status Solidi 248 (1) (2011) 19-27.
- C.M.L. Watts, Xianliang Padilla, J. Willie, Metamaterial electromagnetic wave absorbers, Adv. Mater. 24 (23) (2012) OP98-OP120.
- [36] M.M.K. Hasan, Ajoy, Unesco Chakma, Md Tawhidul Islam, Structural, optical and electronic properties of ZnAg2GeTe4 and ZnAg2Ge0. 93Fe0. 07Te4 photocatalyst: a first principle approach, Mol. Simulat. 47 (7) (2021) 594–601.
- [37] A. Kumer, Unesco, Developing the amazing photocatalyst of ZnAg2GeSe4, ZnAg2Ge0. 93Fe0. 07Se4 and ZnAg2Ge0. 86Fe0. 14Se4 through the computational explorations by four DFT functionals, Heliyon 7 (7) (2021), e07467.
- A.C. Kumer, Unesco, Md Monsur Alam, Purak Chakma, Md Shariful Islam, Nusrat Zahan Khandaker, Tomal Hossain, Al-Nakib Chowdury, Structural, electronic, and opto-electronic properties for BiVS4 photocatalyst effort on wastewater treatment with comparison a standard photocatalyst BiVO4 through the first principles, ECS Trans. 107 (1) (2022), 12109.
- [39] M.M.C. Alam, Unesco, Ajoy Kumer, Md Shariful Islam, Nusrat Zahan Khandaker, Tomal Hossain, Purak Chakma, Jamal Uddin, Investigation of structural, electronic, and optical properties of CdAg2GeSe4 and HgAg2GeSe4 amazing photocatalyst regarding with ZnAg2GeSe4 and a comparative study by DFT functionals, ECS Trans. 107 (1) (2022), 15375.
- [40] K.Y. Ueda, H. Hosono, H. H Kawazoe, Study on electronic structure of CaTiO3 by spectroscopic measurements and energy band calculations, J. Phys. Condens. Matter 11 (17) (1999) 3535.
- [41] L.K. Yu, Robert S, Douglas A. Keszler, Alex Zunger, Inverse design of high absorption thin-film photovoltaic materials, Adv. Energy Mater. 3 (1) (2013)
- [42] N.G. Ravindra, Preethi Choi, Jinsoo, Energy gap-refractive index relations in semiconductors-An overview, Infrared Phys. Technol. 50 (1) (2007) 21-29.
- [43] H.J.H. Queisser, E. Eugene, Defects in semiconductors: some fatal, some vital, Science 281 (5379) (1998) 945-950.
- A.S. Hossain, M.K.R. Khan, M.M. Rahman, Spin effect on electronic, magnetic and optical properties of spinel CoFe2O4: a DFT study, MSI, Mater. Sci. Eng., B 253 (2020), 114496.
- [45] A.M. Jamar, ZAA, W.H. Azmi, M. Norhafana, A.A. Razak, A review of water heating system for solar energy applications, Int. Commun. Heat Mass Tran. 76 (2016)
- [46] W. Tress, Perovskite solar cells on the way to their radiative efficiency limit-insights into a success story of high open-circuit voltage and low recombination, Adv. Energy Mater. 7 (14) (2017), 1602358.
- [47] W.J.F. Royea, Arnel M. Lewis, S. Nathan, Fermi golden rule approach to evaluating outer-sphere electron-transfer rate constants at semiconductor/liquid interfaces. J. Phys. Chem. B 101 (51) (1997) 11152–11159.
- [48] H.B.P. Buckner, H. Nicola, In situ optical absorption studies of point defect kinetics and thermodynamics in oxide thin films, Adv. Mater. Interfac. 6 (15) (2019), 1900496.
- [49] C. Colliex, Electron energy loss spectroscopy in the electron microscope, Adv. Imag. Electron. Phys. 211 (2019) 187-304.
- J.S. Baró, J, J.M. Fernández-Varea, F. Salvat, PENELOPE: an algorithm for Monte Carlo simulation of the penetration and energy loss of electrons and positrons in matter, Nucl. Instrum. Methods Phys. Res. Sect. B Beam Interact. Mater. Atoms 100 (1) (1995) 31-46.
- [51] R.H. Ray, AK, Pintu Sen, Uday Kumar, Manuel Richter, T.P. Sinha, Effects of Octahedral Tilting on the Electronic Structure and Optical Properties of \$ D^ 0\$ Double Perovskites \$\mathbf {\rm A\_2ScSbO\_6} \$(\$\mathbf {\rm A= Sr, Ca} \$), 2013 arXiv preprint arXiv:1310.4853.
- [52] A.E. Babayigit, Anitha, Marc Muller, Bert Conings, Toxicity of organometal halide perovskite solar cells, Nat. Mater. 15 (3) (2016) 247-251.
- [53] I.B. Kyrikou, Demetres, Biodegradation of agricultural plastic films: a critical review, J. Polym. Environ. 15 (2) (2007) 125-150.